Original Research

Insulin resistance induces medial artery calcification in fructose-fed rats

Ye-bo Zhou[1,2], Jing Zhang[3], Yan Cai[4], Xu Teng[4], Xiao-hui Duan[4], Jun-qiu Song[4], Jie Du[1], Chao-shu Tang[1,4] and Yong-fen Qi[1,4]

[1]The Key Laboratory of Remodeling-related Cardiovascular Diseases, Beijing An Zhen Hospital, Capital Medical University, Ministry of Education, Beijing 100029; [2]Department of Physiology, Nanjing Medical University, Nanjing 210029; [3]School of P.E. and Sports Science, Beijing Normal University, Beijing 100875; [4]Key Laboratory of Molecular Cardiovascular Science, Ministry of Education, Beijing 100191, China

Corresponding author: Yong-fen Qi. Email: yongfenqi@yahoo.com

Abstract

Osteogenic differentiation of vascular smooth muscle cells (VSMCs) results in medial artery calcification, which is common in diabetes, but the pathogenesis is poorly understood. We aimed to explore the pathophysiological roles of insulin resistance (IR) on medial artery calcification in rats with 10% fructose in drinking water. After 12 weeks of fructose feeding, rats showed severe IR, with increased levels of fasting blood glucose, serum insulin and oral glucose tolerance test (OGTT). Fructose-fed rats showed aortic calcification, increased aortic calcium deposition and irregular elastic fibers in the medial layer of the vessel wall. Moreover, plasma phosphorus concentration, calcium $\times$ phosphorus product and alkaline phosphatase (ALP) activity, and aortic calcium content and ALP activity were significantly increased. Fructose feeding increased mRNA levels of osteopontin, type III sodium-dependent phosphate co-transporter, bone morphogenetic protein-2 and the key transcription factor core binding factor alpha 1 in aortic tissue and downregulated mRNA levels of osteoprotegerin and matrix γ-carboxyglutamic acid protein. Fructose feeding decreased protein levels of smooth-muscle lineage markers and induced severe lipid peroxidation injury. IR induced by high fructose feeding could evoke osteogenic transdifferentiation of VSMCs and promote vascular calcification.

Keywords: insulin resistance, medial artery calcification, fructose, vascular smooth muscle cells, bone-related protein

Experimental Biology and Medicine 2012; **237**: 50–57. DOI: 10.1258/ebm.2011.011252

Introduction

Vascular calcification (VC) is a well-recognized pathological entity associated with cardiovascular morbidity and mortality.[1] Calcific vasculopathy can be categorized by its location in the neointima (within atherosclerotic plaque) or in the tunica media (the medial smooth muscle layer).[2] Typical atherogenesis is found in large-vessel disease and coronary arteries and is associated with lipid-laden macrophages and intimal hyperplasia. In contrast, medial calcification occurs independent of intimal calcification and atherosclerosis. Medial calcification occurs initially in the medial layer and is not associated with lipid-laden macrophages or intimal hyperplasia. It forms a dense circumferential sheet of calcium crystals in the center of the media, bounded on both sides by vascular smooth muscle cells (VSMCs), and can contain bone trabeculae and osteocytes. Calcification of both locations often occurs in the same patient and even in the same arterial site.

Clinical studies have shown that the index of arterial calcification is significantly higher in diabetic patients than in non-diabetic patients, and the elevated glucose concentrations observed in patients with diabetes may directly affect the calcification process, because patients with diabetes are at increased risk of both atherogenic and medial calcification. A study of 1059 patients with type II diabetes demonstrated that medial arterial calcification of peripheral arteries was a strong independent predictor of total cardiovascular mortality and a significant predictor of future coronary heart disease events, stroke and amputation.[3] Everhart *et al*.[4] showed that risk factors for arterial calcification were impaired vibration perception, long duration of diabetes and high plasma glucose concentration. In calcified distal peripheral arteries from patients with diabetes, VSMCs expressed a number of osteocytic/chondrocytic markers.[5] Despite this strong clinical evidence, a comprehensive explanation for the association of diabetes and medial arterial calcification is still lacking.

VC is an active, cell-regulated process, with many similarities to bone formation.[6–8] Recent studies have shown that VSMCs can lose the expression of smooth-muscle lineage markers and begin to express osteogenic markers and deposit a mineralized bone-like matrix.[6–11] Once the osteogenic phenotype is induced, cells of the vascular wall show a distinctive molecular fingerprint, as indicated by increased levels of bone morphogenetic protein 2 (BMP2) and core binding factor alpha 1 (Cbfα-1).[11–13] Alternatively, loss of endogenous inhibitors of mineralization, such as γ-carboxyglutamic acid (Gla) protein (cMGP) and osteoprotegerin (OPG), also contributes to VC.[13,14]

In this study, we used an insulin-resistant rat model induced by fructose feeding to observe changes in vascular medial calcium and phosphorus contents, alkaline phosphatase (ALP) activity, and the mRNA and protein expression of bone-related protein and lineage markers of VSMCs, and to investigate the mechanisms of VC induced by insulin resistance (IR).

Materials and methods

Materials

Male Sprague–Dawley (SD) rats (180–200 g) were purchased from the Animal Center, Health Sciences Center of Peking University (Beijing, China). All animal care and experimental protocols complied with the Animal Management Rule of the Ministry of Health, People's Republic of China (document no. 55, 2001). Rats were housed under standard conditions (room temperature $20 \pm 8^{\circ}C$, humidity $60 \pm 10\%$, lights from 6:00 to 18:00) and given standard rodent chow and water freely. D-fructose was from Ameresco (Tempe, AZ, USA); kits for ALP, Cu/Zn superoxide dismutase (Cu/Zn SOD) and catalase (CAT) were from Nanjing Jiancheng Bioengineering (Nanjing, China); kits for calcium and phosphorus concentration were from Zhongsheng Biosino Bio-technology and Science (Beijing, China); Trizol was from Gibco-BRL (Rockville, MD, USA); and dNTP, M-MuLV RT, Oligo (dT) 15 primer and Taq DNA polymerase were from Promega (Madison, WI, USA). Oligonucleotides were synthesized by Sai Baisheng Biotechnology (Beijing, China). The sequences of oligonucleotide primers were as follows: osteopontin (OPN)-S, 5′ AGA CCA GCC ATG AGT CAA GTC A 3′ and OPN-A, 5′ TGA AAC TCG TGG CTC TGA TGT T 3′; OPG-S, 5′ TCT ATA CTG CAG CCC CGT GT 3′ and OPG-A, 5′ AGG AGG GCA GCT CCT ATG TT 3′; MGP-S, 5′ AAT CTC ACG AAA GCA TGG AAT C 3′ and MGP-A, 5′ GCA GGC TTG TTG AGT TCC C 3′; BMP2-S, 5′ TCA AGC CAA ACA CAA ACA GC 3′ and BMP2-A, 5′ TGA GCT AAG CTC AGT GGG 3′; type III sodium-dependent phosphate co-transporter (Pit-1)-S, 5′ TGG CTT CTG CTT TAT GGT GGT 3′ and Pit-1-A, 5′ AGG TTC TTC CGA CAA CTG ACC 3′; Cbfα-1-S, 5′ GCC AGG TTC AAC GAT CTG AG 3′ and Cbfα-1-A, 5′ GAG GCG GTC AGA AAC AAA C 3′; β-actin-S, 5′ GAG ACC TTC AAC ACC CCA GCC 3′ and β-actin-A, 5′ TCG GGG CAT CGG AAC CGC TCA 3′. Other chemicals and reagents were of analytical grade.

Preparation of animal model

SD rats were randomly divided into two groups ($n = 12$ each) for treatment for 12 weeks: chow diet and normal drinking water (control) and chow diet and 10% fructose in drinking water (fructose-drinking group).[15] During the last week, all rats underwent a carbohydrate tolerance test.

All rats fasted overnight but had free access to water. At the end of the experiment, rats were anesthetized with ethylcarbamate (10 mg/kg, intraperitoneally). Aortic blood pressure was measured by using a pressure transducer after intubation of a polyethylene catheter (PE-50) filled with heparin through the right carotid artery for 30 min. After measurement of blood pressure, the catheter was maneuvered from the right carotid artery into the left ventricle (LV). Heart rate, left ventricular end-systolic pressure and end-diastolic pressure, left ventricular peak rate of contraction ($+LV\ dp/dt_{max}$) and peak rate of relaxation ($-LV\ dp/dt_{max}$) were measured by using a Power Lab BL-420F instrument (TaiMeng, Chengdu, China). After hemodynamic parameters were measured, a blood sample was drawn and mixed with 1 mg/mL ethylenediaminetetraacetic acid (EDTA)-Na_2 and 500 KIU/mL aprotinin. Plasma was obtained by centrifugation at 3000*g* for 15 min at 4°C and stored at −70°C. The heart and intact aorta were then removed to cold (4°C) phosphate-buffered saline. Hearts were weighed and aortas were stripped of adventitia with the use of sterile forceps. The tissue samples were stored at −70°C.

Fasting blood glucose (FBG) was measured by the glucose oxidase method, and serum insulin concentration was assayed by radioimmunoassay.

Hematoxylin and eosin and von Kossa staining

As described previously,[16] thoracic aortas were fixed in 4% paraformaldehyde for 12 h, embedded in paraffin, then cut into 6 μm-thick sections and stained with hematoxylin and eosin (H&E). A 1-cm segment of aorta was placed in 4% phosphate-buffered neutral formalin (pH 7.4, 0.1 mol/L) for 12 h, immersed in 20% sucrose solution, embedded in optimal cutting temperature compound and then 6-μm-thick frozen sections were cut. The slides were dehydrated before being immersed in a light-protected silver nitrate solution (1 g in 100 mL distilled water) for 30 min under an intense sunbeam, and then immersed in a solution of 5% sodium thiosulfate in distilled water for two minutes. Finally, slides were counterstained with aldehyde-fuchsin and viewed under an Olympus BX50 microscope (Olympus Optical, Tokyo, Japan).

Measurement of calcium and inorganic phosphorus concentrations in plasma and calcium content in aorta

Plasma calcium concentration was measured by the *o*-cresolphthalein colorimetric (OCPC) method of color development to quantify calcium concentration. Plasma samples (0.02 mL) were added into the mixed working reagent solution, including the ethanolamine buffer solution and OCPC and 8-hydroxyquinoline solution, and the ratio

of volume to sample volume was 1:25. The solutions were allowed to stand for five minutes at 30°C. The red absorbance of the compound solution was measured at 600 nm. The detection of inorganic phosphorus in the plasma involved the malachite green direct development process. A 1.0-mL carbamide reagent was added into a 0.02-mL plasma sample with 3.0 mL malachite green molybdic acid reagent and then mixed thoroughly. After 15 min of color development at room temperature (23 ± 1°C), the absorbance was read at 640 nm. The calculation of plasma calcium and phosphorus concentrations followed the kit manufacturer's instructions.

Abdominal aortas (10 mg) were dissolved in HNO_3, then dried in an oven and re-dissolved with the blank solution (27 nmol/L KCl and 27 μmol/L $LaCl_3$). The calcium content was measured by using an atomic absorption spectrophotometer (novAA 300; Analytik Jena AG, Jena, Germany) at 422.7 nm as we described previously.[16] The calcium content of the aorta was normalized to tissue dry weight.

Assay of ALP activity in plasma and aorta

Homogenates of endothelium-denuded thoracic aortas (homogenized buffer: 20 mmol/L HEPES containing 0.2% NP-40 and 20 mmol/L $MgCl_2$) were prepared by using a Polytron (Kinematica Incorporated, Bohemia, NY, USA). After centrifugation at 8000*g* for 10 min, the protein content of the supernatant was determined by the Bradford method.[17] ALP activity was measured by using an ALP assay kit (alkaline buffer:stock substrate solution 1:1). The samples of plasma and supernatant for tissue homogenate of thoracic aortas were mixed with l mL reaction mixture; the mixture was then incubated for 15 min at 37°C. Then the developer (1.5 mL) was added to each well; the red color indicated ALP activity, and the absorbance was determined at 520 nm. ALP activity was calculated according to the manufacturer's instructions. One unit was defined as 1 g tissue protein producing l mg phenol for 15 min.

Measurement of mRNA expression of OPN, OPG, BMP2, MGP, Pit-1 and Cbfα-1

We used reverse transcriptase polymerase chain reaction (PCR) to assess the mRNA expression of OPN, OPG, MGP, BMP2, Pit-1 and Cbfα-1 as described.[18] Total RNA of aortic tissues was extracted by standard techniques, and then quantified by using an ultraviolet (UV) spectrophotometer (Eppendorf AG 22331, Hamburg, Germany). An amount of 2 μg of RNA was primed with Moloney murine leukemia virus and oligo (dT) 15 primer. The PCR reaction mixture was in a 25 μL volume containing 2.5 mmol/L dNTP 1 μL, 10 × PCR buffer 2.5 μL, cDNA 2 μL, 200 nmol/L of the appropriate OPN, OPG, MGP, BMP2, Pit-1 or Cbfα-1 paired primers 1 μL and 1.25 unit Taq DNA polymerase. The following PCR cycles were used: 94°C for 30 s, 57°C for 30 s and 72°C for 40 s, for 30 cycles, then 74°C for five minutes. As an internal control for each PCR reaction, β-actin mRNA was amplified with each sample. A total of 200 nmol/L actin primers and 2 μL cDNA was amplified under the same reaction conditions. All PCR products were loaded onto a 1.5% agarose-Tris-acetate-EDTA gel before electrophoresis, and products were visualized on ethidium bromide staining. The UV illumination photos then underwent computerized densitometric analysis. The final results are expressed as the ratio of OPN, OPG, MGP, BMP2, Pit-1 or Cbfα-1 PCR product to the β-actin PCR product for each sample. All experiments were repeated three times.

Measurement of protein expression of α-actin, SM-22α and β-actin

The rat vessel tissues were prepared by adding a membrane lysis buffer containing a detergent (mmol/L: 16 3-[(3-cholamidopropyl) dimethylammonio]propanesulfonate (CHAPS), 20 Tris-HCl, pH 7.5, 1 Na_2EDTA and 1 dithiothreitol) with protease inhibitors (1 mmol/L benzamidine, 1 μg/mL leupeptin, 10 μg/mL soybean trypsin inhibitor and 0.5 mmol/L phenylmethyl sulfonylfluoride). The samples were then centrifuged at 15,000*g* for 30 min, and the pellets were suspended in lysis buffer. The protein concentration was estimated by the Bradford method.[17] The amount of protein used for Western blot analysis was 20 and 40 μg to detect α-actin and SM-22α, respectively, in rat aortas. The proteins were loaded onto 10% sodium dodecyl sulfate-polyacrylamide gels and underwent electrophoresis and blotting onto nitrocellulose membranes. The membranes were saturated for one hour in Tris buffer solution containing 0.5% Tween and 5% non-fat milk. Then the nitrocellulose membranes were incubated with the primary antibodies anti-α-actin and anti-SM-22α (1:2000) overnight at 4°C, followed by secondary antibody (anti-goat or anti-mouse IgG conjugated to horseradish peroxidase) for one hour, at room temperature. The reaction was visualized by enhanced chemiluminescence. The films were scanned and analyzed by using NIH image software (NIH, Bethesda, MD, USA). The protein contents were normalized to that of β-actin. All experiments were repeated three times.

Measurement of malondialdehyde content and Cu/Zn SOD and CAT activities in aortas

The malondialdehyde (MDA) content was measured by thiobarbituric acid assay. The optical density at 532 nm was measured by using a spectrophotometer. 1,1,3,3-Tetramethoxypropane was used as an external standard, and the level of MDA was expressed as nanomoles per milligram protein for aorta.[19]

Cu/Zn SOD activity was determined by its inhibitory action on the O^2-dependent reduction of xanthine-xanthine oxidase-stimulated ferricytochrome. The assay medium was cytochrome *c*, 100 mmol/L; hypoxanthine, 100 mmol/L; and Tris-HCl (pH 7.4), 10 mmol/L. The reaction was initiated by adding 8 mU xanthine oxidase. The inhibition rate of cytochrome *c* reduction was calculated. SOD activity was expressed as units per milligram protein.

CAT can decompose H_2O_2, and this reaction is stopped by ammonium molybdate. H_2O_2 can bind ammonium molybdate to produce a kind of yellow comoles compound.

Table 1 General characteristics of rats with insulin resistance induced by fructose drinking

	Control	Fructose-drinking
Body weight (g)	488 ± 11	563 ± 12
Fasting blood glucose (mmol/L)	6.18 ± 0.11	7.33 ± 0.35
Fasting blood insulin (mIU/L)	8.37 ± 0.23	17.66 ± 0.69**
HOMA-IR	2.04 ± 0.10	5.18 ± 0.39**
Triglyceride level (mg/dL)	79.47 ± 3.69	162.7 ± 7.28**
Cholesterol concentration (mg/dL)	49.07 ± 1.81	53.79 ± 1.93
LDL-cholesterol concentration (mg/dL)	59.78 ± 2.76	59.89 ± 2.06
HDL-cholesterol concentration (mg/dL)	9.127 ± 0.60	6.63 ± 0.37*

HOMA-IR, homeostasis model assessment of insulin resistance; LDL, low-density lipoprotein; HDL, high-density lipoprotein. Values are mean ± SEM, $n = 10$ in each group
*$P < 0.05$, **$P < 0.01$ versus control

The reduction of H_2O_2 by ammonium molybdate was monitored at 405 nm to measure the amount of yellow comoles compound. One unit of CAT activity is defined as the amount of decomposed H_2O_2 in one milligram vessel tissue for one second. The CAT activity was normalized to the protein content.

Statistical analysis

All statistical analyses were carried out using the GraphPad Prism 5.0 software (GraphPad Software Inc, La Jolla, CA, USA). Data are expressed as mean ± SEM. Comparisons between two groups involved unpaired Student's *t*-test. A two-tailed $P < 0.05$ was considered statistically significant.

Results

Fructose feeding induced IR and mild hypertension

After 12 weeks of 10% fructose administration in drinking water, rats showed no significant differences from controls in body weight. FBG and serum insulin concentrations were greatly increased by 14.1% and 111%, respectively, and the IR index and the total area under the glucose curve were higher by 135% and 40.8% (all $P < 0.01$), respectively, in fructose-fed rats than in control rats (Table 1, Figure 1). In fructose-fed rats, plasma triglyceride concentration was increased 107% ($P < 0.01$) and high-density lipoprotein cholesterol decreased 27.4% ($P < 0.05$) as compared with control rats, with no changes in total cholesterol or low-density lipoprotein cholesterol ($P > 0.05$) (Table 1). Fructose feeding also resulted in mild hypertension, and mean arterial pressure, systolic pressure and diastolic pressure were higher by 23% ($P < 0.01$), 11% ($P < 0.01$) and 14.5% ($P < 0.05$), respectively, than in control rats (Table 2). Left ventricular systolic pressure was increased by 10.9% ($P < 0.05$) as compared with control rats.

Fructose feeding induced vascular calcification

Histological sections of fructose-fed aortas showed more proliferative smooth muscle cells and local hyperplastic structure with irregular elastic fibers in the aortic medial layer (Figure 2). Von Kossa staining revealed dispersed calcified nodules among the elastic fibers in calcified aortas (Figure 3); the aortic calcium concentration and ALP activity were significantly increased by 3.52- and 3.28-fold (all $P < 0.01$), respectively, as compared with controls. Plasma phosphorus concentrations, calcium × phosphorus (Ca × P) product and ALP activity were increased by 47.5%, 50.2% and 66.7% ($P < 0.01$), respectively (Table 3).

Fructose feeding increased the aortic mRNA level of OPN, pit-1, BMP2 and Cbfα-1 and decreased that of OPG and MGP

OPN, Pit-1, BMP2 and Cbfα-1 mRNA levels were higher in aortic tissue by 69.8% ($P < 0.01$), 69.1% ($P < 0.05$), 93.1% ($P < 0.01$) and 90.2% ($P < 0.05$), respectively, in fructose-fed rats than in control rats, whereas fructose feeding

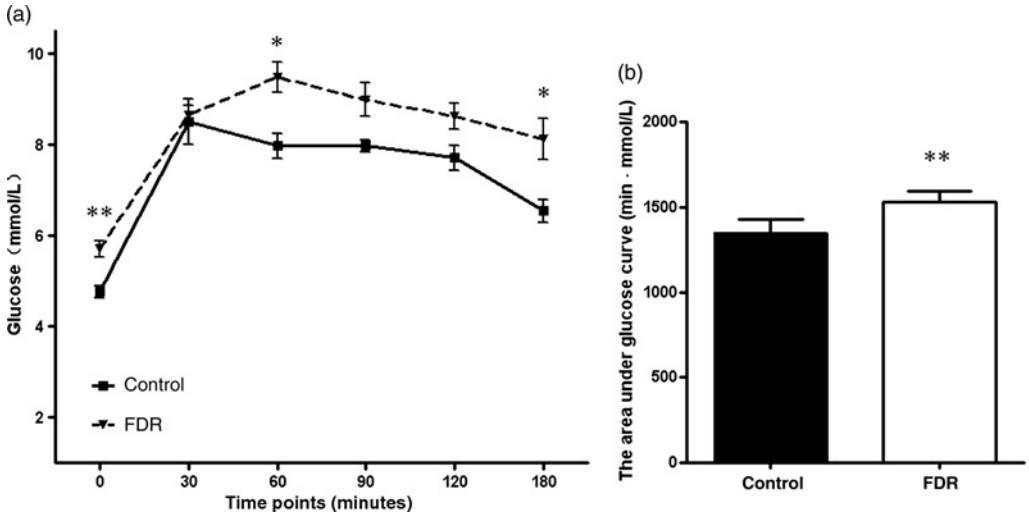

Figure 1 Glucose responses during the oral glucose tolerance test (OGTT) of the 12-week fructose drinking: (a) the glucose curve and (b) the total area under the glucose curve. FDR, fructose-drinking rats. Data are mean ± SEM. $n = 10$. *$P < 0.05$, **$P < 0.01$ versus control

Table 2 Effect of fructose drinking on heart rate, blood pressure and heart function in rats

	Control	Fructose-drinking
LVW/BW (mg/g)	2.33 ± 0.15	2.24 ± 0.11
HR (beats/min)	334 ± 11	369 ± 15
MAP (mmHg)	74 ± 3	91 ± 3**
SAP (mmHg)	109 ± 3	121 ± 3**
DAP (mmHg)	62 ± 3	71 ± 2*
LVSP (mmHg)	110 ± 4	122 ± 3*
LVEDP (mmHg)	−11.6 ± 0.78	−12.0 ± 0.99
+LV dp/dt_{max} (mmHg/s)	4635 ± 149	4747 ± 137
−LV dp/dt_{max} (mmHg/s)	−3718 ± 110	−3787 ± 97

LVW, left ventricular weight; BW, body weight; HR, heart rate; MAP, mean arterial pressure; SAP, systolic aortic pressure; DAP, diastolic aortic pressure; LVSP, left ventricular systolic pressure; LVEDP, left ventricular end diastolic pressure; ± LV dp/dt_{max}, left ventricular peak rate of contraction and peak rate of relaxation were measured *in vivo*. Values are mean ± SEM, $n = 10$ in each group. *$P < 0.05$, **$P < 0.01$ versus control

downregulated the mRNA expression of OPG and MGP by 46.1% and 43.6% ($P < 0.01$), respectively (Figure 4).

Fructose feeding resulted in loss of lineage markers in VSMCs

Because the phenotype transition of VSMCs is associated with VC *in vitro* and *in vivo*, we further investigated the protein expression of smooth-muscle lineage markers. Compared with normal vessels, fructose-fed vessels showed decreased protein concentration of α-actin and SM-22α by 27.9% and 43.5% (all $P < 0.01$), respectively (Figure 5).

Fructose feeding promoted oxidative stress

Fructose feeding induced severe lipid peroxidation injury: MDA content in aorta was increased by 183% ($P < 0.05$), and SOD and CAT activity were reduced by 46.1% and 61.1% (all $P < 0.01$), respectively (Table 4).

Discussion

VC is common in subjects with diabetes mellitus and is considered an important risk factor of cardiovascular morbidity and mortality with diabetes.[20] Clinical and pathophysiological studies have shown severe coronary artery calcification, a typical intimal calcification, associated with diabetes.[21,22] In fact, radiologically detectable medial calcification in peripheral arteries or abdominal aorta are strong prognosticators of future cardiovascular events in patients with type 2 diabetes.[23] Further studies showed morphological and molecular differences between atherosclerotic and medial calcification.[23] However, most of the mechanisms that drive medial calcification in IR are still incompletely understood.

In the present study, we found that SD rats fed 10% fructose in drinking water for 12 weeks showed mild hypertension, IR, hyperinsulinemia and hyperglyceridemia, as was previously shown.[24] Compared with the control group, fructose-fed rats showed aortic calcification, as shown by von Kossa staining for calcification, increased aortic calcium deposition and irregular elastic fibers in the medial layer of the vessel wall. Moreover, plasma phosphorus concentration, Ca × P product and ALP activity,

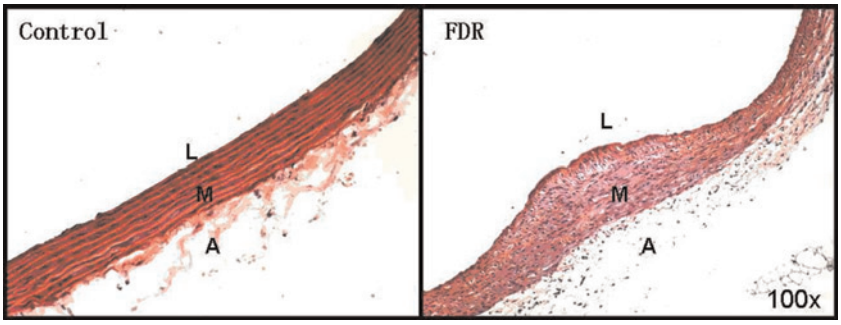

Figure 2 Effect of fructose drinking on structure of the thoracic aorta of rats with calcification ($n = 6$/group, original magnification ×100 for all staining sections). Sections were stained with hematoxylin/eosin. FDR, fructose-drinking rats; L, lumen; M, media; A, adventitia. (A color version of this figure is available in the online journal)

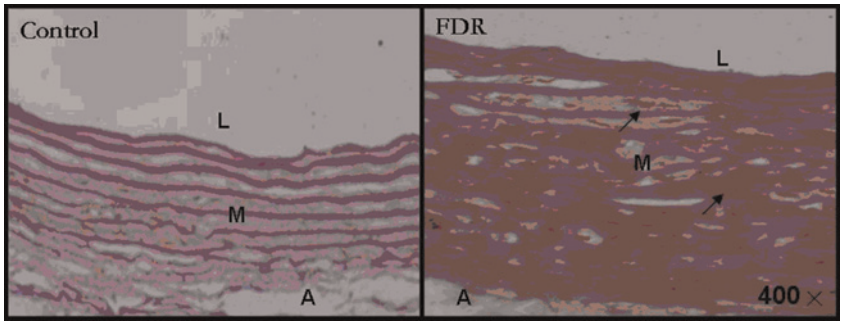

Figure 3 Effect of fructose feeding on calcific nodules in thoracic aortas of rats with calcification ($n = 6$/group, original magnification ×400 for all von Kossa-stained sections). Arrows show calcified nodules. FDR, fructose-drinking rats; L, lumen; M, media; A, adventitia. (A color version of this figure is available in the online journal)

Table 3 Effect of fructose drinking on plasma ionized calcium (Ca) and phosphorus (P) concentrations, Ca × P product and alkaline phosphatase (ALP) activity, and aortic calcium content and ALP activity in rats

	Control	Fructose-drinking
Plasma Ca concentration (mg/dL)	9.04 ± 0.31	9.18 ± 0.35
Plasma P concentration (mg/dL)	3.93 ± 0.14	5.80 ± 0.22**
Plasma Ca × P product (mg^2/dL^2)	35.47 ± 1.52	53.26 ± 2.86**
Plasma ALP activity (U/L)	35.05 ± 0.84	58.43 ± 2.52*
Aortic Ca content (μmol/g dw)	51.13 ± 1.96	231.0 ± 8.66**
Aortic ALP activity (U/g protein)	93.16 ± 3.96	398.4 ± 16.41**

Ca, calcium; P, phosphorous; dw, dry weight. Values are mean ± SEM, $n = 10$ in each group. *$P < 0.05$, **$P < 0.01$ versus control

and aortic calcium content and ALP activity were significantly increased, which suggests that IR induces aorta calcification in fructose-fed rats. Ample evidence suggests that promoting osteogenic transition of contractile VSMCs is related to VC.[9,11,12] Thus, arterial calcification is considered associated with a loss of smooth-muscle lineage markers and a gain of an osteogenic phenotype, as indicated by increased expression of bone-related protein. In the present study, we found strikingly decreased levels of SM-22α and α-actin and increased expression of OPN, BMP2, Pit-1 and Cbfα-1 in calcified vascular aortas of fructose-fed rats. Inhibitory bone-regulated protein such as OPG and MGP are necessary to prevent soft-tissue calcification.[6] MGP is thought to be an inhibitor of VC because of its Ca^{2+}-binding γ-carboxyglutamic acid (Gla) motif,[25,26] inhibition of cartilage calcification[27] and binding to and antagonizing BMP2 to prevent osteogenic transition of contractile VSMCs.[28,29] OPG is a secreted protein of the tumor necrosis factor family; targeted deletion of the OPG gene resulted in calcification of the aorta and renal arteries in mice.[30,31] We found the mRNA levels of OPG and MGP significantly decreased in fructose-fed rats, which may further enhance VC.

Several mechanisms may regulate the expression of bone-related protein of VSMCs in IR. Recent papers investigated the effect of high glucose and high insulin on the SMC phenotype *in vitro* and their contribution to calcification. High glucose induced the expression of ALP and osteocalcin in bovine SMCs, which was accompanied by an increase in calcium deposition.[32] In *in vitro* studies, high glucose induced cell proliferation and expression of OPN in cultured rat VSMCs[33] and in medial layers of the carotid arteries of streptozotocin-induced diabetic rats.[34] More recently, high

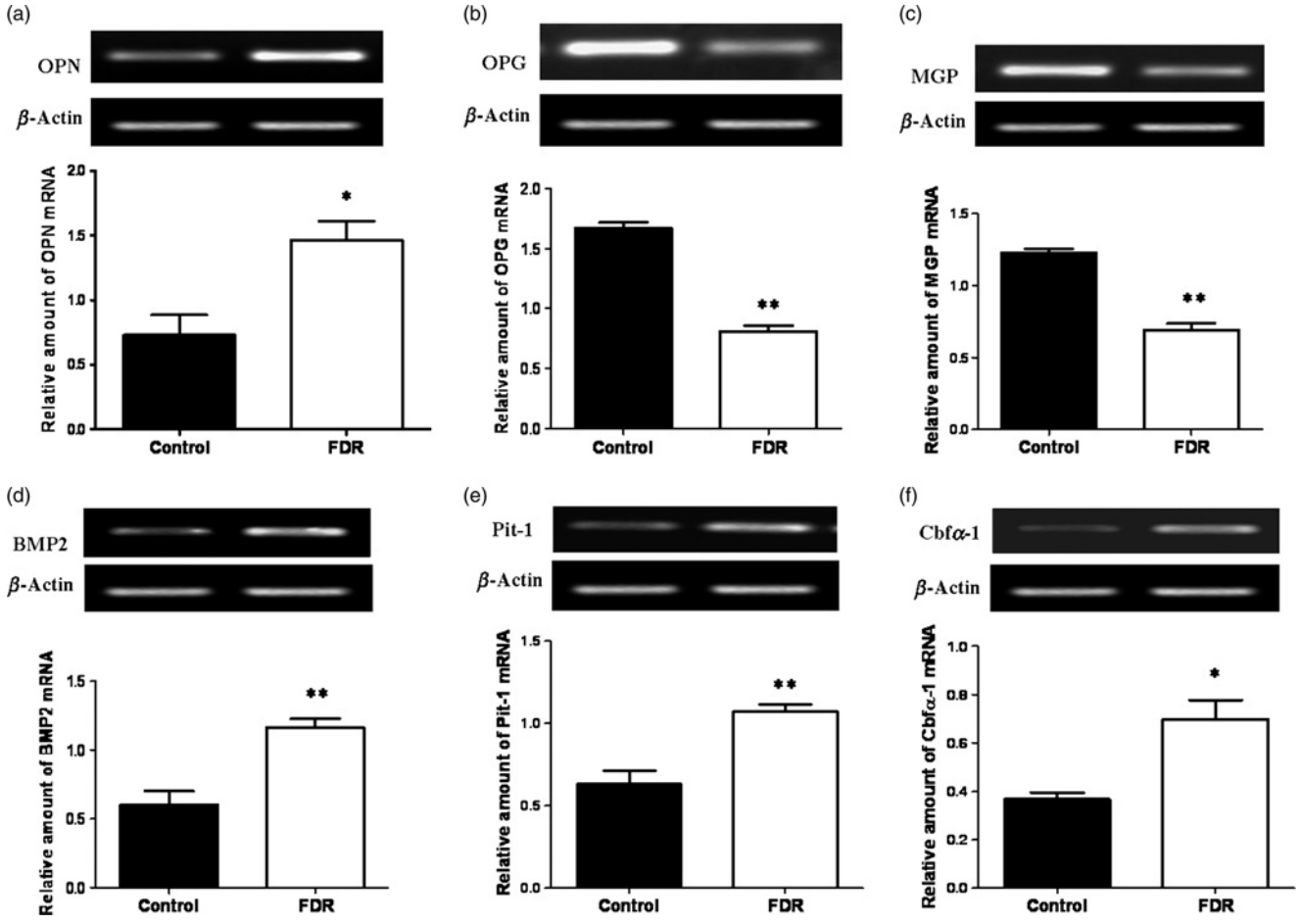

Figure 4 Reverse transcriptase polymerase chain reaction analysis of effect of fructose on the mRNA expression of (a) osteopontin (OPN), (b) osteoprotegerin (OPG), (c) matrix γ-carboxyglutamic protein (MGP), (d) bone morphogenetic protein 2 (BMP2), (e) type III sodium-dependent phosphate co-transporter (Pit-1) and (f) core binding factor alpha 1 (Cbfα-1) in aortas of rats. FDR, fructose-drinking rats. Data are mean ± SEM from three independent experiments and were normalized to β-actin expression *$P < 0.05$, **$P < 0.01$ versus control

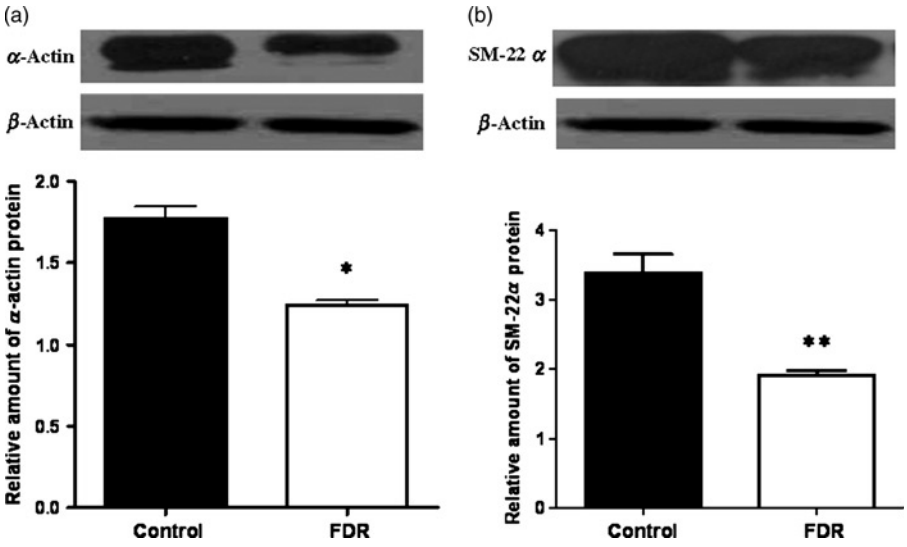

Figure 5 Western blot analysis of effect of fructose on the protein expression of (a) α-actin and (b) SM-22α in aortas of rats. FDR, fructose-drinking rats. Data are mean $\pm$ SEM from three independent experiments and were normalized to β-actin protein concentrations. $^{*}P < 0.05$, $^{**}P < 0.01$ versus control

Table 4 Effect of fructose on aortic superoxide dismutase (SOD), catalase (CAT) activity and malondialdehyde (MDA) concentrations in rats

	Control	Fructose-drinking
SOD activity (U/mg protein)	148.4 $\pm$ 8.73	79.9 $\pm$ 3.19**
CAT activity (U/mg protein)	54.87 $\pm$ 3.62	21.3 $\pm$ 1.44**
MDA (μmol/g protein)	1.17 $\pm$ 0.07	3.3 $\pm$ 0.17**

Values are mean $\pm$ SEM, $n = 10$ in each group
$^{**}P < 0.01$ versus control

insulin was found to accelerate calcium deposition in human VSMCs, which was accompanied by decreased synthesis of OPG.[31] High concentrations of glucose with insulin treatment increased [^{3}H]-thymidine uptake, ALP activity, and the number of mineralized nodules and area stained for collagen in bone-marrow stromal cells,[35] which suggests that insulin can promote osteoblast proliferation and function. Therefore, both high glucose and high insulin may be added to the list of factors promoting VC. Our study revealed that high fructose feeding induced hyperglycemia and hyperinsulinemia, which could increase ALP activity and the mRNA expression of BMP-2, Cbfα-1, OPN and Pit-1 and downregulate the expression of OPG and MGP, which are critical for the pathogenesis of VC because these osteoblast-like cells can then regulate the production of the matrix and subsequent calcification.[36,37]

In addition to hyperglycemia and hyperinsulinemia, oxidative stress plays a critical role in VC. Liu *et al*.[38] showed that oxysterol cholestane-3β, 5α, 6β-triol (Triol) increased calcifying nodule formation, calcium deposition and ALP activity in calcifying VSMCs, which were all attenuated by antioxidant vitamin C plus vitamin E. Triol promoted VSMC calcification probably by a reactive oxygen species (ROS)-related mechanism. Oxidative stress is closely linked to apoptosis and can alter both signal transduction and genomic processes.[39] Bovine retinal pericyte apoptosis induced by advanced glycation end products was found associated with decreased cellular CAT and SOD activities and increased MDA production, which is similar to antioxidant results in patients with diabetes.[40] Oxidative stress parameters were observed in a fructose-fed-induced IR model, and high fructose feeding was associated with an early (one week) increase in ROS production by the aorta, heart and circulatory polymorphonuclear cells[41] associated with enhanced markers of oxidative stress. We revealed that fructose feeding increased lipid peroxidation and inhibited the activity of antioxidases such as SOD and CAT, which may be involved in the pathogenesis of VC.

Our fructose feeding-induced IR resulted in medial artery calcification, significantly altered mRNA expression of aortic bone-related proteins and strikingly decreased protein expression of VSMC lineage markers in the tunica media of vessel walls. High fructose feeding-induced hyperglycaemia and hyperinsulinemia and increased oxidative stress may be involved in medial artery calcification.

Author contributions: All authors participated in the design, interpretation of the studies and analysis of the data and review of the manuscript. Y-fQ and C-sT designed the study and wrote the paper; Y-bZ, YC, XT, X-hD and J-qS performed the research; and JZ and JD analyzed the data. Y-bZ and JZ contributed equally to the work.

ACKNOWLEDGEMENTS

This work was supported by The Program for New Century Excellent Talents in University, Education Ministry of China (grant no. NCET-05-0016) and the National Natural Science Foundation of China (grant nos. 30470693, 30871013).

REFERENCES

1 Shaw LJ, Raggi P, Berman DS, Callister TQ. Coronary artery calcium as a measure of biologic age. *Atherosclerosis* 2006;**188**:112–9
2 Sage AP, Tintut Y, Demer LL. Regulatory mechanisms in vascular calcification. *Nat Rev Cardiol* 2010;**7**:528–36

3 Lehto S, Niskanen L, Suhonen M, Ronnemaa T, Laakso M. Medial artery calcification. A neglected harbinger of cardiovascular complications in non-insulin-dependent diabetes mellitus. *Arterioscler Thromb Vasc Biol* 1996;**16**:978–83

4 Everhart JE, Pettitt DJ, Knowler WC, Rose FA, Bennett PH. Medial arterial calcification and its association with mortality and complications of diabetes. *Diabetologia* 1988;**31**:16–23

5 Shanahan CM, Cary NR, Salisbury JR, Proudfoot D, Weissberg PL, Edmonds ME. Medial localization of mineralization-regulating proteins in association with Monckeberg's sclerosis: evidence for smooth muscle cell-mediated vascular calcification. *Circulation* 1999;**100**:2168–76

6 Johnson RC, Leopold JA, Loscalzo J. Vascular calcification: pathobiological mechanisms and clinical implications. *Circ Res* 2006;**99**:1044–59

7 Shao JS, Cai J, Towler DA. Molecular mechanisms of vascular calcification: lessons learned from the aorta. *Arterioscler Thromb Vasc Biol* 2006;**26**:1423–30

8 Demer LL, Tintut Y. Vascular calcification: pathobiology of a multifaceted disease. *Circulation* 2008;**117**:2938–48

9 Steitz SA, Speer MY, Curinga G, Yang HY, Haynes P, Aebersold R, Schinke T, Karsenty G, Giachelli CM. Smooth muscle cell phenotypic transition associated with calcification: upregulation of Cbfa1 and downregulation of smooth muscle lineage markers. *Circ Res* 2001;**89**:1147–54

10 Tyson KL, Reynolds JL, McNair R, Zhang Q, Weissberg PL, Shanahan CM. Osteo/chondrocytic transcription factors and their target genes exhibit distinct patterns of expression in human arterial calcification. *Arterioscler Thromb Vasc Biol* 2003;**23**:489–94

11 Moe SM, Duan D, Doehle BP, O'Neill KD, Chen NX. Uremia induces the osteoblast differentiation factor Cbfa1 in human blood vessels. *Kidney Int* 2003;**63**:1003–11

12 Cola C, Almeida M, Li D, Romeo F, Mehta JL. Regulatory role of endothelium in the expression of genes affecting arterial calcification. *Biochem Biophys Res Commun* 2004;**320**:424–7

13 Engelse MA, Neele JM, Bronckers AL, Pannekoek H, de Vries CJ. Vascular calcification: expression patterns of the osteoblast-specific gene core binding factor alpha-1 and the protective factor matrix gla protein in human atherogenesis. *Cardiovasc Res* 2001;**52**:281–9

14 Luo G, Ducy P, McKee MD, Pinero GJ, Loyer E, Behringer RR, Karsenty G. Spontaneous calcification of arteries and cartilage in mice lacking matrix GLA protein. *Nature* 1997;**386**:78–81

15 Renna N, Risler N, Cruzado M, Gonzalez S, Lama C, Miatello RM. Effect of nebivolol on cardiovascular changes associated with a rat model of insulin-resistance. *Cell Mol Biol* 2005;**51**:531–7

16 Zhou YB, Jin SJ, Cai Y, Teng X, Chen L, Tang CS, Qi YF. Lanthanum acetate inhibits vascular calcification induced by vitamin D3 plus nicotine in rats. *Exp Biol Med* 2009;**234**:908–17

17 Bradford MM. A rapid and sensitive method for the quantitation of microgram quantities of protein utilizing the principle of protein–dye binding. *Anal Biochem* 1976;**72**:248–54

18 Qi YF, Bu DF, Niu da D, Shi YR, Wang SH, Pang YZ, Tang CS, Du JB. Effects of different peptide fragments derived from proadrenomedullin on gene expression of adrenomedullin gene. *Peptides* 2002;**23**:1141–7

19 Askawa T, Matashushita S. Thiobarbituric acid test for detecting lipid peroxide. *Lipids* 1979;**14**:401–6

20 Rydén L. What are the risk factors for progression of coronary artery calcification in patients with type 2 diabetes? *Nat Clin Pract Cardiovasc Med* 2008;**5**:370–81

21 Ahmadi N, Tirunagaram S, Hajsadeghi F, Flores F, Saeed A, Hecht H, Naghavi M, Budoff M. Concomitant insulin resistance and impaired vascular function is associated with increased coronary artery calcification. *Int J Cardiol* 2010;**144**:163–5

22 Heinonen SE, Leppänen P, Kholová I, Lumivuori H, Häkkinen SK, Bosch F, Laakso M, Ylä-Herttuala S. Increased atherosclerotic lesion calcification in a novel mouse model combining insulin resistance, hyperglycemia, and hypercholesterolemia. *Circ Res* 2007;**101**:1058–67

23 Qiao JH, Mertens RB, Fishbein MC, Geller SA. Cartilaginous metaplasia in calcified diabetic peripheral vascular disease: morphologic evidence of enchondral ossification. *Hum Pathol* 2003;**34**:402–7

24 Hwang IS, Ho H, Hoffman BB, Reaven GM. Fructose-induced insulin resistance and hypertension in rats. *Hypertension* 1987;**10**:512–6

25 Price PA, Urist MR, Otawara Y. Matrix Gla protein, a new gammacarboxyglutamic acid-containing protein which is associated with the organic matrix of bone. *Biochem Biophys Res Commun* 1983;**117**:765–71

26 Hackeng TM, Rosing J, Spronk HM, Vermeer C. Total chemical synthesis of human matrix Gla protein. *Protein Sci* 2001;**10**:864–70

27 Yagami K, Suh JY, Enomoto-Iwamoto M, Koyama E, Abrams WR, Shapiro IM, Pacifici M, Iwamoto M. Matrix GLA protein is a developmental regulator of chondrocyte mineralization and, when constitutively expressed, blocks endochondral and intramembranous ossification in the limb. *J Cell Biol* 1999;**147**:1097–108

28 Sweatt A, Sane DC, Hutson SM, Wallin R. Matrix Gla protein (MGP) and bone morphogenetic protein-2 in aortic calcified lesions of aging rats. *J Thromb Haemost* 2003;**1**:178–85

29 Bostrom K, Tsao D, Shen S, Wang Y, Demer LL. Matrix GLA protein modulates differentiation induced by bone morphogenetic protein-2 in C3H10T1/2 cells. *J Biol Chem* 2001;**276**:14044–52

30 Bucay N, Sarosi I, Dunstan CR, Morony S, Tarpley J, Capparelli C, Scully S, Tan HL, Xu W, Lacey DL, Boyle WJ, Simonet WS. Osteoprotegerin-deficient mice develop early onset osteoporosis and arterial calcification. *Genes Dev* 1998;**12**:1260–8

31 Olesen P, Nguyen K, Wogensen L, Ledet T, Rasmussen LM. Calcification of human vascular smooth muscle cells: associations with osteoprotegerin expression and acceleration by high-dose insulin. *Am J Physiol Heart Circ Physiol* 2007;**292**:H1058–64

32 Chen NX, Duan D, O'Neill KD, Moe SM. High glucose increases the expression of Cbfa1 and BMP-2 and enhances the calcification of vascular smooth muscle cells. *Nephrol Dial Transplant* 2006;**21**:3435–42

33 Sodhi CP, Phadke SA, Batlle D, Sahai A. Hypoxia stimulates osteopontin expression and proliferation of cultured vascular smooth muscle cells: potentiation by high glucose. *Diabetes* 2001;**50**:1482–90

34 Mori S, Takemoto M, Yokote K, Asaumi S, Saito Y. Hyperglycaemia-induced alteration of vascular smooth muscle phenotype. *J Diabetes Complications* 2002;**16**:65–8

35 Gopalakrishnan V, Vignesh RC, Arunakaran J, Aruldhas MM, Srinivasan N. Effects of glucose and its modulation by insulin and estradiol on BMSC differentiation into osteoblastic lineages. *Biochem Cell Biol* 2006;**84**:93–101

36 Moe SM, Chen NX. Pathophysiology of vascular calcification in chronic kidney disease. *Circ Res* 2004;**95**:560–7

37 Giachelli CM. Vascular calcification mechanisms. *J Am Soc Nephrol* 2004;**15**:2959–64

38 Liu H, Yuan L, Xu S, Zhang T, Wang K. Cholestane-3beta, 5alpha, 6beta-triol promotes vascular smooth muscle cells calcification. *Life Sci* 2004;**76**:533–43

39 Du X, Stotcklauser-Farber K, Rosen P. Generation of reactive oxygen intermediates, activation of NF-kappaB, and induction of apoptosis in human endothelial cells by glucose: role of nitric oxide synthase? *Free Radic Biol Med* 1999;**27**:752–63

40 Chen B, Jiang D, Tang L. Advanced glycation end-products induce apoptosis involving the signaling pathways of oxidative stress in bovine retinal pericytes. *Life Sci* 2006;**79**:1040–8

41 Delbosc S, Paizanis E, Magous R, Araiz C, Dimo T, Cristol JP, Cros G, Azay J. Involvement of oxidative stress and NADPH oxidase activation in the development of cardiovascular complications in a model of insulin resistance, the fructose-fed rat. *Atherosclerosis* 2005;**179**:43–9

(Received July 19, 2011, Accepted October 6, 2011)